GROW: A Global Time Series Dataset for Groundwater Studies within the Earth System

Annemarie Bäthge[1*], Claudia Ruz Vargas[2], Gunnar Lischeid[3,4], Raoul Collenteur[5], Mark Cuthbert[6], Jan Fleckenstein[7], Martina Flörke[8], Inge de Graaf[9], Sebastian Gnann[10], Andreas Hartmann[11], Xander Huggins[12], Nils Moosdorf[13,14], Yoshihide Wada[15], Thorsten Wagener[4], Robert Reinecke[1]

[1]Institute of Geography, Johannes Gutenberg-University, Mainz, Mainz, Germany
[2]International Groundwater Resources Assessment Centre (IGRAC), Delft, The Netherlands
[3]Research Area 4: "Simulation & Data Science", Leibniz Centre for Agricultural Landscape Research, Müncheberg, Germany
[4]Institute of Environmental Science and Geography, University of Potsdam, Germany
[5]Department Water Resources and Drinking Water, Eawag, Dübendorf, Zürich, Switzerland
[6]School of Earth and Environmental Sciences, Cardiff University, UK
[7]Department of Hydrogeology, Helmholtz Center for Environmental Research, Leipzig, Germany
[8]Institute of Engineering Hydrology and Water Resources Management, Ruhr University Bochum, Bochum, Germany
[9]Earth Systems and Global Change group, Wageningen University and Research, Wageningen, the Netherlands
[10]Chair of Hydrology, University of Freiburg, Freiburg, Germany
[11]Institute of Groundwater Management, Dresden University of Technology
[12]Institute for Resources, Environment, and Sustainability, University of British Columbia, Vancouver, BC, Canada
[13]Leibniz Centre for Tropical Marine Research (ZMT), Bremen, Germany
[14]Kiel University, Kiel, Germany
[15]Biological and Environmental Science and Engineering Division, King Abdullah University of Science and Technology, Thuwal, Saudi Arabia
* Correspondence: a.baethge@uni-mainz.de

ABSTRACT

Groundwater is a central component of the Earth system. However, our understanding of how it is dynamically interlinked with the atmosphere, hydrosphere, cryosphere, biosphere, geosphere, and anthroposphere remains limited. In the pursuit of understanding groundwater dynamics across diverse global settings, we present GROW (global integrated GROundWater package). This analysis-ready, quality-controlled dataset combines depth to groundwater and level time series from around the world with associated Earth system variables. The dataset contains > 180,000 time series from 41 countries, with either daily, monthly, or yearly temporal resolution, accompanied by 35 time series or attributes of meteorological, hydrological, geophysical, vegetation, and anthropogenic variables (e.g., precipitation, drainage density, aquifer type, NDVI, land use). 33 data flags regarding well features (e.g., location coordinates and country), as well as time series characteristics (e.g., gap fraction or length), facilitate quick data filtering. GROW provides a foundation for understanding large-scale groundwater processes in space and time, as well as for calibrating and evaluating models that simulate groundwater dynamics within the Earth system.

BACKGROUND AND SUMMARY

Access to groundwater is pivotal for humans and ecosystems that depend on it as a freshwater source[1–3]. Groundwater is the largest store of unfrozen freshwater on Earth, accounting for approximately 99% of the Earth's accessible freshwater[3]. It is estimated to contribute between 19% (PCR-GLOBWB, period 2000-2015[4]) and 22% (WaterGAP v2.2e, period 1991 – 2019[5]) to the total global water withdrawal use**.** Beyond its role as a source for anthropogenic water consumption, groundwater plays a key role for biodiversity as it sustains various ecosystems, especially phreatophytic vegetation in drylands, surface waters, and wetlands[6]. Saccò et al.[2] estimated that 75 % of the habitable land area is ecologically interconnected with groundwater. Ecosystems that rely on groundwater, also called groundwater-dependent ecosystems[7], provide multiple benefits by regulating climate, floods, water quality, hosting biodiversity and having recreational and cultural value[2,8].

While critical to humans and ecosystems, groundwater accessibility is threatened by anthropogenic activity-driven changes in hydrological storages and fluxes. Among others, groundwater accessibility is limited by the depth of the water table. When water tables decline, groundwater may become inaccessible for anthropogenic water supply[9] and groundwater-dependent ecosystems[6]. Rohde et al.[6] showed that 53% of groundwater-dependent ecosystems in drylands are at risk because of declining water tables. One of the biggest threats is over-abstraction, which has led to widespread groundwater depletion[3,10,11]. Based on estimations for 2010, 70% of global groundwater abstraction was attributed to irrigational water use[1]. The pressure that irrigation exerts on groundwater accessibility was recently highlighted by Jasechko et al.[12] who found that aquifer systems with water tables in rapid decline are most common in agricultural drylands. Consequently, it is not surprising that the water scarcity hotspots in the world occur in many arid and semiarid regions, like Pakistan, northeastern China and the Middle East, where groundwater withdrawal for irrigation is prevalent[11,13]. Humans further impact water tables through land use changes, e.g., urbanization, wetland loss and conversion to agricultural land[11,14,15] which in turn changes infiltration[16], interception, evapotranspiration[17], runoff[14] and recharge due to irrigation that is fed by surface waters[11,17]. Additionally, climate change and its consequences alters the water cycle in manifold ways (e.g., soil moisture depletion[18], sea level rise[18,19], melting of glaciers, and thawing of permafrost[17]). However, the quantification of this impact on groundwater systems remains uncertain[3,20–22].

To predict how these threats and changes will affect water table dynamics and how we can mitigate and adapt to their impacts, we need to investigate groundwater as an integral part of the Earth system[23–26]. Accomplishing this requires groundwater not to be studied in isolation but in combination with environmental variables within the Earth system (here referred to as Earth system variables) to determine their interactions with and influence on groundwater. By doing so, controls behind water table dynamics can be addressed and their respective importance compared[24]. Groundwater's embeddedness within the Earth system suggests that its dynamics may be shaped more by the configuration of multiple Earth system variables across these interconnected systems than by individual system properties[27]. We understand that the Earth system is not only composed of natural components like the atmosphere, geosphere, hydrosphere, cryosphere, and biosphere[28] but also includes the anthroposphere[14].

In Table 1, we present relationships of groundwater within different Earth system components that have been identified as crucial for quantitative groundwater dynamics. The selection of the Earth system variables is rooted in existing literature and limited due to data availability. To provide a clear overview, the Earth system variables are categorized into six components: atmosphere (1), geosphere (2), hydrosphere (3), cryosphere (4), biosphere (5), and anthroposphere (6).

Table 1: Overview of prominent relationships that highlight groundwater's interconnectedness within the Earth system. For each Earth system component, the associated Earth system variables included in GROW are listed. More information about the Earth system variables is given in Table 3 & 4 and the dataset documentation on Zenodo. Some Earth system variables can be related to multiple components but are only named in one. The listed literature on relationships with groundwater is exemplary and does not represent a systematic literature review spanning all processes within an Earth system component.

Earth system component + Earth system variables in GROW	**Relationship with groundwater**
(1) Atmosphere + Precipitation + Potential evapotranspiration + Actual evapotranspiration + Air temperature + Koeppen-Geiger classification + Hydrobelt	• Precipitation controls the amount of atmospheric water that is available to replenish groundwater[29–31]. • In the case of a bidirectional connection of atmosphere and groundwater, water is lost to the atmosphere by actual evapotranspiration[32,33]. • Precipitation and potential evapotranspiration together form temporal (seasons) and spatial (climate zones) gradients along which groundwater recharge patterns emerge[24,34–36]. • Air temperature dictates the capacity of ambient air to hold water vapor. With higher air temperature, the saturation vapor pressure increases, and more water is present in gaseous form. By that, potential evapotranspiration can increase with temperature[37]. Air temperature also affects processes such as vegetation growth and snow accumulation, which in turn impact groundwater processes (see (4), (5)).

(2) Geosphere + Ground elevation + Topographic slope + Rock type + Permeability + Total porosity + Aquifer type + Saturated hydraulic conductivity for topsoil and subsoil + Soil texture class for topsoil and subsoil	• Topography is a core driver of groundwater flow, where discharge areas develop within topographic lows[38,39]. • Topographic slope influences the partitioning of water into groundwater recharge. Steeper slopes can promote less diffuse recharge because water moves overland and downhill rather than percolating[30,33]. On the other hand, steeper slopes are also related to deep infiltration and deep groundwater flow paths[39,40]. • Groundwater is stored in and flows through pores and fractures of geological layers[41]. Geological properties like permeability and porosity strongly influence groundwater flow, response time[32,33,42] and storage capacity[43]. • Soil characteristics like permeability, among others determined by soil texture, affect capillary rise and the percolation of water[30,33]. With larger sand fractions in soil, permeability and consequently recharge usually increase[33,44].
(3) Hydrosphere + Distance between perennial streams + Drainage density	• Groundwater buffers surface water level fluctuations and may sustain streamflow during dry periods[11,17,45]. • Infiltration from surface waters is often the main source of groundwater recharge in drylands[29,45].
(4) Cryosphere + Permafrost cover + Glacier cover + Snow depth	• In cold regions, soil may be permanently frozen (permafrost), which inhibits groundwater recharge[46], groundwater flow and groundwater-surface water connectivity[17]. • Where surface catchments are (partly) covered with glaciers, their meltwater can be an important source of recharge[47]. • In snowy climates, snow cover accumulates during cold periods and is released during melt, delaying the recharge response[23,31,48].
(5) Biosphere + Interception loss + NDVI + Leaf area index – low vegetation + Leaf area index – high vegetation + Groundwater-dependent ecosystems	• Vegetation affects interception[33], transpiration, and soil structure[30,33,49], thereby determining the water fluxes to and from groundwater. It is generally accepted that high vegetation density is associated with reduced groundwater recharge[30,44], but this can change under specific settings (e.g., dry tropical regions)[50]. • Groundwater supplies the soil root zone with water and can serve as a reliable water source in dry climates[38,51]. As a result, the water table can regulate the depth of plant roots and biomass[52]. • Where vegetation roots are directly abstracting from groundwater (phreatophytes), their health is sensitive to water table fluctuations[53].
(6) Anthroposphere + Total water withdrawal for industrial and domestic use + Land use fraction of rainfed cropland, irrigated cropland,	• Groundwater withdrawal can lead to short-term or persistent decline of water tables[9,45]. • Land use practices like surface water-fed irrigation, forest clearance or urbanization can influence groundwater recharge[33].

pastures, forests & natural vegetation and urban areas + Main land use + Groundwaterscapes

The general understanding of the complex interconnectedness of groundwater within the Earth system is still incomplete[17,20,54]. This knowledge gap includes a lack of observations in environments like high-latitudes[17,30] and regions without agricultural influence[27], a lack of knowledge regarding environmental characteristics like the spatial heterogeneity of hydraulic conductivity in subsurface catchments[55,56] and insufficient knowledge about measurement errors[57]. Modeling is not only constrained by the uncertainty regarding processes and state variables, particularly evident for input and boundary conditions, but also by oversimplification of processes and the lack of clarity regarding the optimal implementation of them in models[54,54,57,58]. These limitations contribute to highly uncertain groundwater simulations[17,58].

In situ measurements are key to closing this knowledge gap[17,23,59] because a reliable set of measured data can be used to analyze drivers behind groundwater dynamics[17,23,60]. This enhances our integrated process understanding of groundwater within the Earth system[60] and, consequently, can lead to improved conceptual/perceptual models that can be implemented in computational models. Other than that, global models could highly benefit from global time-varying groundwater datasets for parametrization and model evaluation[58]. A dataset built for these purposes should:

(1) be a **global dataset** that captures the natural variability of the included variables, which enables better intercomparison between regions[61] and helps reveal large-scale processes and connections[3,11,23,62]. It can be used to develop, calibrate, and evaluate large-scale hydrological, land-surface, and climate models[54,59,63];

(2) contain **time series data** that provide insights into temporal patterns (e.g., seasonality), extreme events, and cause-effect lags[3,14,58,64];

(3) combine groundwater observations with **associated variables of the Earth system** that can be used to explain groundwater dynamics[23,30,65]. Huggins et al.[60] emphasized that there is an underrealized potential in combining existing groundwater and Earth system data to uncover relationships that have not yet been recognized;

(4) include **metadata** to improve comparability and the assessment of data uncertainty according to best practices in large-sample datasets[20,54,61];

(5) be **standardized** and **freely available** according to the FAIR principles to enhance applicability and accessibility[60,61,66].

A dataset that fulfills most of these aspects is CARAVAN[63]. It combines regional collections of measured daily streamflow time series with meteorological forcing data from ERA5-Land[67] and catchment attributes from HydroAtlas[68]. CARAVAN is a best-practice dataset for streamflow studies but contains no in-situ groundwater time series. There are datasets that have been developed to understand quantitative groundwater dynamics. Regional sets of groundwater level time series accompanied with additional environmental information exist, e.g., for Chile[26], Switzerland[69] or the Baltic countries[70]. But a comparison of these datasets without extensive preprocessing is difficult as they are standardized differently and contain different variables. At the global scale, static datasets such as Fan et al.[62] with depth to groundwater and Moeck et al.[30] with groundwater recharge provide steady-state groundwater records for many locations worldwide. The Global Groundwater Monitoring Network (GGMN)[71] contains groundwater level or depth time series from different regions of the world, but lacks an extensive set of associated Earth system variables. Consequently, past studies that analyzed observational data have either focused on steady-state data[35,38], which can only be used to a limited extent to understand temporal patterns. Others have concentrated on regional[65,72,73] to continental scales[29,74], but their results are not able to capture teleconnections, global interlinkages[54], and the diversity of environmental settings in which groundwater occurs. Jasechko et al.[12] made substantial progress by analyzing temporally dynamic groundwater level data on a global scale, focusing on time series with yearly resolution and exploring the influence of two variables—aridity index and land under cultivation—on observed trends. Still, this leaves potential for more comprehensive studies, integrating more timescales and a wider set of Earth system variables.

As there is currently no dataset that meets all the needs for an extensive groundwater analysis, we developed GROW (global integrated GROundWater package), a quality-controlled dataset that accompanies depth to groundwater and level time series from around the world with associated Earth system variables. GROW is designed to enable large-sample spatiotemporal groundwater analysis without further preprocessing, making it "analysis-ready." The groundwater data included in GROW has been checked for records that indicate measurement errors and gaps. Duplicate time series and wells with erroneous coordinates were discarded. Harmonization to a daily, monthly, or yearly temporal resolution ensures equal time step intervals. Overall, GROW contains 187,317 time series. The median depth to groundwater computed over all time series is 8 m. 59% of the time series are at least 10 years long, and nearly all records are situated within North America, Europe, or Australia (> 90%). 62% of the time series show no significant trend (p-value > 0.05), while 26% show a decreasing and 12% increasing water table. Covering all major Earth system components, the groundwater data are accompanied by 35 groundwater-associated variables (time series and attributes) that are categorized into: atmosphere (n=6), geosphere (10), hydrosphere (2), cryosphere (3), biosphere (5) and anthroposphere (9) (see also Table 1). 33 data flags related to well features (e.g., location coordinates, country), as well as time series characteristics (e.g., time series length, trend direction, autocorrelation, total gap fraction), enable targeted filtering.

With GROW, we offer a database to the global community that can be used to understand spatiotemporal groundwater dynamics in the context of the Earth system. Cumulative effects of multiple controls on groundwater time series can be studied in space and time. Processes conceptualized for specific environmental settings can be transferred to regions with no data but the same environmental conditions. Especially tools like machine learning[59,75] and principal component analysis[76] have the potential to uncover hidden connections in large datasets. In addition to this, the harmonized groundwater time series in GROW provide a ready-to-use calibration and validation dataset for global hydrological, land-surface, or climate modeling. We not only encourage hydrologists to use the dataset but also experts and scientists from other fields, as groundwater dynamics feed back into other storages and fluxes of the Earth system.

METHODS

Groundwater time series

The groundwater time series in GROW were derived from the global groundwater datasets *Global Groundwater Monitoring Network (GGMN)*[71] and *Other data*[77] hosted by the *International Groundwater Resources Assessment Centre*. These datasets were used because they are the most comprehensive and publicly available collection of observed groundwater time series currently available. Among others, groundwater time series from the study of Jasechko et al.[12] are partially included in *Other data*. The two datasets together contain 221,123 time series (as of June 2024) and have heterogeneous temporal scales and reference point elevations. The groundwater records of a time series are either given as depth from the ground elevation to groundwater (97%), depth from the top of the well to groundwater (0.004%), or groundwater level elevation above mean sea level (3%). We do not label the groundwater data as hydraulic head because of the following reasons. The depth to groundwater records would need to be transferred to groundwater level elevation, but the ground elevation is only specified by the data provider for 20% of the depth to groundwater time series. Other than that, the information on whether the aquifer is confined or unconfined is only provided for 6.5% of the time series and an estimation is not possible with the available data. For readability, we use water table as a term in the rest of the article when referring to both depth to groundwater and groundwater level records; this does not affect the published data, which contains both variables. In addition to the time series, static attributes are provided for each well, including coordinates, country, data license, confinement, and more.

The preprocessing of the time series data consists of nine steps, as outlined in Table 2 (steps 1 - 9). In addition, attribute data were checked for duplicates and erroneous coordinates (Table 2; steps 10 - 13). Examples of discarded or flagged time series are provided in Supplements section S1. In close cooperation and in parallel to the development of GROW, IGRAC addressed the following issues that were identified during preprocessing: In the updated versions of *GGMN* and *Other data* (1) negative depth to groundwater records were interrogated and verified to distinguish between correct values (in the case of flowing artesian wells), incorrect signing and measurement errors (incorrect signing was found and corrected) (Table 2, step 3) and (2) time series duplicates by coordinates, starting date, ending date and mean water table were removed (Table 2, step 10b).

Table 2: Overview of preprocessing steps for the groundwater data, including the number and percentage of discarded/flagged time series and the flags created per step. All data flags are listed in Table 5.

Preprocessing step	Percentage and (number) of discarded (D) or flagged (F) timeseries	Created data flag Complete list in Table 5
1. Discarding time series with less than 2 records Empty records and duplicates are removed. In this study, time series are defined as containing a minimum of two records at different timestamps. This criterion is checked at the start and after every preprocessing step in which data is aggregated or discarded. Empty or one-record time series are discarded.	D: 8.22% (18,175) F: 0	
2. Reconciling records to ensure that only one groundwater reference point elevation is provided per time series Records with more than one reference point in the same time series exist. 2.7% of the time series contain both depth to groundwater and groundwater level records. To ensure consistency and comparability, groundwater level records are removed from these time series. This is because most records in these cases are given as depth to groundwater (86%), and the level is usually additionally provided with a timestamp that already contains depth to groundwater information.	D: < 0.01% (11) F: 0	
3. Removing negative depth to groundwater and -999/-9,999 records Depth to groundwater records that are negative, indicating that the hydraulic head is above ground, naturally exist in the case of flowing artesian wells[78] or riparian zones[79]. However, we are unable to manually check all > 180,000 wells to distinguish plausible negative records from potential measurement errors. Therefore, negative depth to groundwater records are removed as potential measurement errors. However, time series with records that are completely negative are kept. In their case, we assume that the sign was incorrectly transmitted by the organisation and switch it as a correction. Because the entries "- 999" and "- 9,999" are common to mark missing records and are below realistic value ranges, they are removed from groundwater level.	D: 0.08% (166) F: 0	

4. Temporal aggregation of time series to either daily, monthly, or yearly resolution		
In the original data, a timestamp is provided for each record. However, it is unknown whether the water table was measured at that specific timestamp or if it represents the mean over a specific day, month, or year (which is mostly likely the case when the dates are provided as the zeroth hour or the first day of the year or month). For more straightforward analysis, the temporal resolution is harmonized to ensure equal time step intervals. The time series are aggregated to either daily, monthly, or yearly resolution. The classification is based on the 75th percentile of the intervals between the timestamps. If this interval is shorter than 2 days, the time series is harmonized to a daily resolution. If it is between 2 and 41 days, it is averaged to a monthly resolution. 41 days is chosen as the upper threshold because some time series have a loose monthly schedule, including record intervals between 20 and 40 days. The remaining time series are aggregated to yearly means. For transparency, the number of records aggregated to the daily, monthly, or yearly means is flagged in cases where time series do not solely contain the first day of the month [year] (e.g., 2010-01-01) or the zeroth hour of the day (e.g., 2010-01-01 00:00:00). In latter case, we assume that the records already represent aggregated means of multiple records whose number is unknown (aggregated_from_n_values = "NA").	D: 0.89% (1,957) F: 83% YS (154,627), 11% MS (21,443), 6% d (11,247) F: 62% not-NA (116,530)	 ***interval*** [d,MS,YS] ***aggregated_from_n_values*** [number]
5. Capping the gap fraction and gap length		
GROW provides an additional data field for every time series where gaps are linearly filled. To minimize the impact of the gap-filling on the statistical characteristics of the time series, the total gap fraction and gap length are capped accordingly:		
a. The maximum allowed gap length is set as 6 days for daily data, 3 months for monthly data, 1 year for yearly data between 3 and 9 years long, and one year more for every additional 5 years up to 4 years for time series that are 20 years or longer. We selected these thresholds so that the gap lengths are not longer than 20% of a month (daily data), year (monthly data) or the total length of the time series (yearly data). To account for natural variance within time series, the individual allowed gap length can be smaller when a time series has a high scattering. Based on the autocorrelation of every time series, the allowed gap between	D: 1.59% (3,526) F: 22% True (146,133)	 ***autocorrelation*** [True/False]

two steps is determined to be the maximum time lag for which the autocorrelation is equal to or larger than 0.6 (spearman rank correlation coefficient[80]), considering only time lags up to the point where the correlation coefficient becomes negative for the first time. Still, the maximum gap length is the upper limit. If there is no autocorrelation exceeding 0.6 within the considered time lags, no gaps are allowed. The sequence is extracted in which the gaps do not exceed the individual gap length threshold, and the preprocessing is continued. b. The total allowed gap fraction is 20%. For time series that exceed this threshold, the longest sequence of years with less than 20% gaps is extracted for daily and monthly data. For yearly data, only the sequence without gaps is extracted.	D: 1.55% (3,436) F: 100% not-NA	***gap_fraction*** [number]
6. Flagging high-magnitude water table jumps >= 50 m as potential measurement error		
High-magnitude water table changes (jumps) in time series can result from sensor failures. However, this can also be attributed to the natural variance of highly dynamic aquifers, weather extremes, or anthropogenic pumping. As we are not aware of an algorithm which can distinguish between large jumps caused by sensor failure and realistic circumstances (including rare events), we decided to use a threshold that is so high (>= 50 m) and rare (appears only 1-2 times in a time series) that it is unlikely to be explained by natural conditions or anthropogenic interferences. Consequently, the entire time series is flagged as likely to contain measurement errors when the water table jumps by 50 m or more between two adjacent time steps, and this occurs no more than twice.	D: 0 F: 0.33% True (720)	***jumps*** [True/False]
7. Flagging uninterrupted sequences of the exact same water table as potential measurement error		
Uninterrupted sequences of the exact same water table (plateaus) are flagged in each time series with their plateau length. The same thresholds are chosen for the plateaus as for the maximum gap length, meaning that, for example, a plateau is defined as 7 days or longer for daily data. Like the jumps-flagging, this indicates possible measurement errors.	D: 0 F: 3.54% True (7,830) F: 100% not-NA	Attribute table: ***plateaus*** [True/False] Time series table: ***plateaus*** [plateau length in time steps]
8. Calculating Mann-Kendall trend direction and Sen's slope		

The trend direction and the Sen's slope, in case of a significant trend (p-value < 0.05), were derived for each time series. If the time series was flagged to be autocorrelated (see step 4), the Hamed and Rao Modified Mann-Kendall test was used to perform the trend analysis. Here, a variance correction is applied to account for serial autocorrelation[81]. Otherwise, the original Mann-Kendall test from the python package pyMannKendall was utilized[82]. The trend direction for time series containing depth to groundwater records was switched (increasing <-> decreasing) so that, for example, a rising water table (decreasing depth) is flagged as "increasing". Additionally, the sign of the trend slope is switched for these cases. It should be noted that the effect size and significance of a test should be critically scrutinized because of its dependence on sample size[83].	D: 0 F: 62% no trend (115,879), 26% decreasing (48,749), 12% increasing (22,689) F: 38% not-NA (71,438)	***trend_direction*** ["no trend", "increasing", "decreasing"] ***trend_slope*** [m/year]
9. Adding further data flags		
Additional flags were generated per time series and added to the well attributes.	D: 0 F: 100% not-NA	**starting_date** [date] **ending_date** [date] **length_years** [number] **aggregated_from_n_values_median** [number] **groundwater_mean_m** [number] **groundwater_median_m** [number]
10. Removing duplicates in well attributes		
There are two types of duplicates apparent in the dataset. Duplicate by well ID and country (a), and duplicate by location and groundwater time series (with different ID; b):		
a. To assign the attributes to the time series a unique key in every table is necessary. As time series and attributes in the source data were sorted in different folders by country, the well ID and country can be used to merge the data. Consequently, duplicate records with duplicate ID from the same country are both deleted as it is not feasible to resolve which IDs should be assigned to each time series.	D: 0.05% (105) F: 0	
	D: 0.33%	

b. Furthermore, wells with the same coordinates, starting date, ending date and mean water table under two different IDs were identified as duplicates. In this case, only one well record was removed.	(731) F: 0
11. Checking for coordinates outside the plausible range	
The coordinates of the well location are projected in WGS 84. In this coordinate system, the latitude must be between -90° and 90°, and the longitude between -180° and 180°. Outliers are removed from the dataset as a manual data correction is not feasible for such a large dataset.	D: 2.58% (5,698) F: 0
12. Removing empty attribute columns	
23 empty columns were removed.	D: 0 F: 0
13. Trimming time series based on kept attributes	
Time series whose well attributes were lost during the preprocessing (step 10-11) were removed.	See step 10 and 11

Earth system variables

The scope of the dataset and the selection of Earth system variables added to GROW are based on a selection of processes most relevant to water table dynamics (see Table 1). To expand the groundwater time-series data with these variables, data products were identified that fulfil the following criteria. (1) The data product must be published under a license that permits modification and redistribution. (2) Instead of using multiple regional data products per variable, only global data products were considered to enable comparability within GROW. (3) When choosing between different data products, preference was given to data products based on the following priorities (in decreasing order): greater temporal coverage, outperforming comparable data products as indicated in the literature, higher temporal resolution, and higher spatial resolution. (4) Furthermore, variables and data products were chosen that could either be downloaded automatically or did not need extensive preprocessing.

In total, thirty-five Earth system variables were selected to complement the groundwater attributes and time series. The added Earth system variables were derived from observation-based data, reanalysis data, or modelled data. Table 3 (attributes) and Table 4 (time series) give an overview of every variable and its source. They are categorized into the six Earth system components (Table 1).

It is desirable to associate groundwater time series with precipitation and potential evapotranspiration records as comprehensive as possible as these are widely recognized to be the most important, large-scale, non-anthropogenic variables driving groundwater dynamics[12,35,69,74]. To increase temporal coverage and account for some uncertainty in precipitation and potential evapotranspiration data products, two complementary products per variable were added to GROW, each one as separate column. The MSWEP 3-hour precipitation data product[84] merged multiple precipitation data sources (gauge-measurements, satellite, or reanalysis) and selected per location that data source with the highest quality. MSWEP has a high temporal resolution and can cover the most recent groundwater records as it is almost updated in real-time with a latency of 3 hours. Following this, we selected this product due to its high data quality standards, high temporal resolution, and coverage of the most recent records. However, it does not cover records before 1979. Early groundwater records are therefore supplemented with monthly precipitation data from GPCC[85], which can cover records before 1901 (begins in 1891) and have a higher spatial resolution (0.25°) in comparison to other products that start before 1901 like Observed Land Surface Precipitation Data (2.5°)[86]. Both datasets cover 99.99% of the groundwater time series, while only one of them (MSWEP) achieves a record coverage of 98% (Table 4). Regarding potential evapotranspiration, ERA-5 Land data[67] cover the longest time span (1950-2024) but are known to overestimate potential evapotranspiration[37,87], especially for arid regions[67]. To account for this uncertainty, we include another product derived from a different data source. The Global land evaporation Amsterdam model (GLEAM4) was selected because it calculates potential evapotranspiration with Penman's equation[88] unlike ERA5-Land, whose potential evapotranspiration is simulated with a land surface model "for agricultural land as if it is well watered and assuming that the atmosphere is not affected by this artificial surface condition"[67].

To merge the Earth system variables with each groundwater well, the value of the raster pixel or polygon containing the well's location is extracted and associated with that well. This means that the variables are not measured at the explicit location of a well, but are, due to the nature of raster or polygon data, averaged over a certain region. With this in mind, the results should be understood as local to regional characteristics, representative for the respective spatial resolutions of the Earth system variables (with a spatial resolution range from 3 arc seconds to 0.5°, Table 3 & 4). Since the well coordinates are projected in WGS 84, the used data products were reprojected to WGS 84 if they were initially available in a different coordinate system. The static variables (no temporal dimension) were added as columns in the attributes table. The time series variables were first aggregated to the temporal scale of each individual groundwater time series and merged by ID and date to the time series table.

Some variables were only available at monthly (precipitation from GPCC) or yearly resolutions (water withdrawal and land use fractions). We include these data also for daily and monthly time series as they can be used to split the dataset based on thresholds. Therefore, these products are combined with daily [monthly] data so that each day [month] within a specific month [year] is matched with the corresponding value for that month [year].

The time series with different temporal resolutions are stored in a single table, all with the same unit of quantity (mm/year) for parameters such as precipitation. This enables the straightforward derivation of further aggregations across different time series resolutions, subsets, and statistics, regardless of the temporal resolution. Because 83% of the time series have a yearly resolution, quantitative units are provided for an annual period (mm/year). This means that monthly and daily time series also have units of mm/year.

In the following, we briefly describe the processing steps needed for a few variables that require additional processing:

- The aquifer type [porous, fractured, porous/fractured, karst and water_body] was estimated based on the World Karst Aquifer Map (WOKAM)[89] and the GLiM[90]. Wells, which are located in a WOKAM-karstifiable region, are assigned "karst" as aquifer type. For the rest of the wells the following classification based on GLiM rock types was applied. The aquifer type is porous when the rock type is unconsolidated sediments (GLiM class: su). As aquifers in mixed sedimentary rocks and siliciclastic sedimentary rocks (GLiM class: sm,ss) can be porous or fractured, wells within those rock types are assigned “porous/fractured”. The class “water body” is directly transferred from GLiM’s class “water bodies”. The rest is classified as fractured.

- Drainage density was calculated by dividing the sum of all river lengths in a catchment by the area of that catchment. HydroRIVERS[91] and BasinATLAS (level 9)[68] were utilized for that purpose. Both datasets were reprojected into the global metric coordinate system World-Eckert-IV before calculating the fraction of river lengths sum per basin area. This step leads to a higher spatial distortion towards the north and south pole. Regarding the basins, in which groundwater wells are located, the median discrepancy between the basin area indicated by BasinAtlas and the area calculated in World-Eckert-IV is 0.82 km². 192 basins are affected by a very large distortion of 10 km² or more (maximum of 1,228,275 km²). To account for this, the drainage density is assigned as missing for basins where the area discrepancy is equal or larger than 10 km².
- The main land use type in the attributes table is that land use whose average fraction over time is the highest.

Table 3: Overview of all added Earth system attributes (no temporal dimension), their data source and characteristics. Record coverage refers to the percentage of wells in GROW's attributes table that contain a value for that variable.

Earth system variable	Column name in GROW	Earth system component	Data source	Spatial resolution	Original Unit	Unit in GROW	Record coverage
Koeppen-Geiger classification	koeppen_geiger_class	Atmosphere	CHELSA v2.1 - kg0[92]	30 arc sec	/	/	100%
Hydrobelt	hydrobelt_class	Atmosphere & Hydrosphere	Meybeck et al. 2013[93]	*polygons*	/	/	90%
Ground elevation	ground_elevation_m_asl	Geosphere	MERIT DEM[94]	3 arc sec	m	m	100%
Topographic slope	topographic_slope_degree	Geosphere	Geomorpho90m[95]	7.5 arc sec	°	°	>99%
Rock type	rock_type_0-100_m_class	Geosphere	GLiM[90]	0.5°	/	/	96%
Aquifer type	aquifer_type_class	Geosphere	WHYMAP WOKAM[89] + GLiM[90]	*polygons* + 0.5°	/	/	97%
Permeability for 0-100 m depth	permeability_0-100_m_m-2	Geosphere	GLHYMPS2.0[96]	*polygons*	m^2	m^2	>99%
Total porosity for 0-100 m depth	total_porosity_0-100_m_fraction	Geosphere	GLHYMPS[43]	*polygons*	/	/	>99%
Soil texture class in topsoil (0-30 cm)	soil_texture_0-30_cm_class	Geosphere	HiHydroSoil[97]	250 m	/	/	>99%
Soil texture class in subsoil (30-200 cm)	soil_texture_30-200_cm_class	Geosphere	HiHydroSoil[97]	250 m	/	/	64%

Saturated hydraulic conductivity of topsoil (0-30 cm)	soil_saturated_conductivity_ 0-30_cm_cm_d-1	Geosphere	HiHydroSoil[97]	250 m	cm/ day	cm/ day	>99%
Saturated hydraulic conductivity of subsoil (30-200 cm)	soil_saturated_conductivity_ 30-200_cm_cm_d-1	Geosphere	HiHydroSoil[97]	250 m	cm/ day	cm/ day	>99%
Distance between perennial streams	distance_perennial_ streams_m	Hydrosphere	Cuthbert, Gleeson et al.[74] - 0.1 cubic metres per second flow threshold	1 km	m	m	>99%
Drainage density	drainage_density_m-1	Hydrosphere	HydroRivers[91] + BasinATLAS Level 9[68]	*polygons + polylines*	m^{-1}	m^{-1}	99%
Glacier cover in surface catchment	glacier_cover_fraction	Cyrosphere	BasinATLAS Level 9[68]	*polygons*	/	/	>99%
Permafrost cover in surface catchment	permafrost_cover_fraction	Cyrosphere	BasinATLAS Level 9[68]	*polygons*	/	/	>99%
Groundwater dependent ecosystems	groundwater_dependent_ ecosystems_class	Biosphere	Huggins et al.[98]	30 arc sec	/	/	100%
Main land use	main_land_use_class	Anthroposphere	Volkholz & Ostberg 2024[99]	0.5°	/	/	>99%
Groundwaterscapes	groundwaterscapes_ID_class	Integrates multiple components	Huggins et al. 2024[27]	5 arc min	/	/	93%

Table 4: Overview of all added time-varying Earth system variables, their data source, and characteristics. Record coverage refers to the percentage of records in GROW's time series table that contain a value for that variable.

Earth system variable	**Column name in GROW**	**Earth system component**	**Data source**	**Spatial resolution**	**Temporal resolution**	**Temporal coverage**	**Original Unit**	**Unit in GROW**	**Record coverage**
Precipitation	precipitation_gpcc__mm_year-1	Atmosphere	GPCC[85]	0.25°	monthly	1891-2020	mm/ month	mm/ year	85%
Precipitation	precipitation_mswep__mm_year-1	Atmosphere	MSWEP V2[84]	0.25°	3-hourly	1979-2024	mm/ 3 hours	mm/ year	98%
Potential Evapo-transpiration	potential_evapotranspiration_era5_mm_year-1	Atmosphere	ERA5-Land[100,101]	0.08°	daily	1950-2024	mm/ day	mm/ year	97%
Potential Evapo-transpiration	potential_evapotranspiration_gleam_mm_year-1	Atmosphere	GLEAM4[88]	0.25°	daily	1980-2023	mm/ day	mm/ year	90%
Actual Evapotranspiration	actual_evapotranspiration_mm_year-1	Atmosphere	GLEAM4[88]	0.25°	daily	1980-2023	mm/ day	mm/ year	90%
Air temperature	air_temperature_C°	Atmosphere	ERA5-Land[100,101]	0.08°	daily	1950-2024	K	°C	97%
Snow depth	snow_depth_m	Cyrosphere	ERA5-Land[100,101]	0.08°	daily	1950-2024	m	m	97%
Interception loss	interception_mm_year-1	Biosphere	GLEAM4[88]	0.25°	daily	1980-2023	mm/ day	mm/ year	90%
NDVI	ndvi_ratio	Biosphere	1981-2013: AVHRR NDVI[102]; 2014-2024: VIIRS NDVI[103]	0.05°	daily	1981-2024	/	/	93%
Leaf area index of low vegetation	lai_low_vegetation_ratio	Biosphere	ERA5-Land[100,101]	0.08°	daily	1950-2024	/	/	53%
Leaf area index of high vegetation	lai_high_vegetation_ratio	Biosphere	ERA5-Land[100,101]	0.08°	daily	1950-2024	/	/	74%

Withdrawal for industrial use	withdrawal_industrial _m3_year-1	Anthropos-phere	Wada et al.[104]	0.5°	yearly	1901 - 2021	m^3/ year	m^3/ year	91%
Withdrawal for domestic use	withdrawal_domestic_ m3_year-1	Anthropo-sphere	Wada et al.[104]	0.5°	yearly	1901 - 2021	m^3/ year	m^3/ year	91%
Fraction of urban areas	urban_area_fraction	Anthropo-sphere	Volkholz & Ostberg[99]	0.5°	yearly	1901 - 2021	/	/	91%
Fraction of pastures	pastures_fraction	Anthropo-sphere	Volkholz & Ostberg[99]	0.5°	yearly	1901 - 2021	/	/	91%
Fraction of rainfed cropland	cropland_rainfed_ fraction	Anthropo-sphere	Volkholz & Ostberg[99]	0.5°	yearly	1901 - 2021	/	/	91%
Fraction of irrigated cropland	cropland_irrigated_ fraction	Anthropo-sphere	Volkholz & Ostberg[99]	0.5°	yearly	1901 -2021	/	/	91%
Fraction of forests and natural vegetation	forests_natural_ vegetation_fraction	Anthropo-sphere	Volkholz & Ostberg[99]	0.5°	yearly	1901 -2021	/	/	91%

DATA RECORDS

The final GROW dataset consists of two files: A table containing time series data and a table with static attribute data. Both can be downloaded as either a comma-separated values (.CSV) or .parquet file from Zenodo: (*link will be provided in peer-reviewed manuscript*) and used under a Creative Commons Attribution Non-Commercial ShareAlike 4.0 International License (CC-BY-NC-SA 4.0). A dataset documentation on Zenodo (Readme file) provides descriptions of every variable/column for both tables. To subset the data, the attributes table can be filtered based on user-specified criteria, and afterwards the time series table can be filtered for the remaining well IDs in the attributes table. A total of 33 data flags are available to help with this filtering (Table 5). With quality flags like "aggregated_from_n_values", "jumps", and "plateaus", users can select data based on their individual quality needs. For example, a data subset is possible in which yearly data was either not aggregated (always the first day of the year) or aggregated from at least four values. To provide another example, a user can decide to drop all time series that contain jumps (0.33% of the time series) or plateaus (3.54% of the time series). A best-practice script for data selection can be viewed on GitHub (*link will be provided in peer-reviewed manuscript*) or Zenodo: (*link will be provided in peer-reviewed manuscript*).

Table 5: List of all data flags that are added to the time series and attributes table. [The flags in brackets] were already part of the GGMN and "Other data" datasets.

Data flags in time series table	**Data flags in attributes table**
• interval (d, MS, YS) • year (e.g., 2008) • month (e.g., 2008-02) • aggregated_from_n_values [e.g., 1] • plateaus (length of plateau in time steps, e.g., 10)	• interval (d, MS, YS) • starting_date (e.g., 2010-01-01) • ending_date (e.g., 2013-03-08) • length_years (in years, e.g., 9) • autocorrelation (True, False) • aggregated_from_n_values_median (e.g., 2) • gap_fraction (e.g., 0.1) • jumps (True, False) • plateaus (True, False) • trend_direction (no trend, increasing, decreasing) • trend_slope_m_year-1 (e.g., 0.9) • groundwater_mean_m (e.g., 34) • groundwater_median_m (e.g., 34) [feature type, purpose, status, description, latitude, longitude, surface_elevation_m_asl, top_of_well_ elevation_m_asl, country, address, license, aquifer_name, confinement, organisation, manager, drilling_total_depth_m, parameter (renamed to "reference point")]

A map showing the global distribution of the wells included in GROW (Figure 1) highlights the geographic patterns in data availability. This mapping reveals a bias to locations within North America, Europe, and Australia, which contain over 90% of the data records. With a median depth to groundwater of 8 m, GROW represents shallow groundwater (here defined with depth to groundwater below 10 m like in Cuthbert et al.[74]), whereby monthly (5 m) and yearly (7 m) time series have even shallower median depth to groundwaters. While the earliest time series starts in 1835, the year in which the highest number of time series begin is 2002 (10.7%). The year 2010 has the greatest data availability, with a total count of 110,938 time series. 39% of the time series are between 10 and 19 years long (73,579). 20% of the time series are 20 years and longer (37,163) with a maximum length of 135 years. Time series of 20 years and longer are more common to have a yearly resolution (90%) compared to all time series (83%). On the other hand, short time series of 1 to 4 years have the highest fraction of daily (14%) and monthly (29%) resolution time series among the length classes. Figure 1 also shows the number of time series with no significant trend ($p > 0.05$) in the water table (115,879; 62%), a decreasing trend (48,738; 26%), and an increasing trend (22,700; 12%).

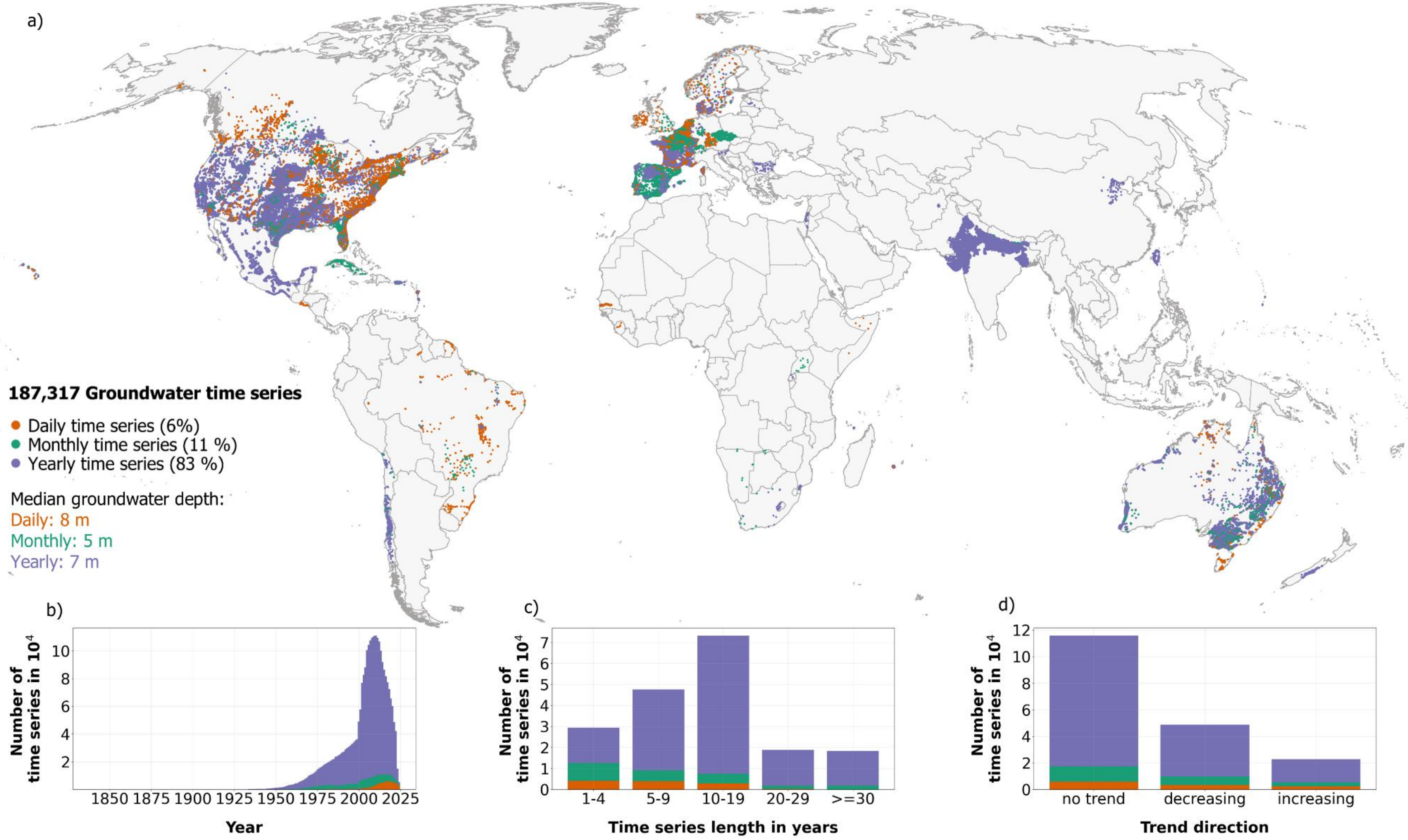

Figure 1- Locations of all time series, classified by temporal resolution (a). *The color indicates whether a time series has a daily (orange), monthly (green) or yearly (purple) resolution. Additionally, the median depth to groundwater per well is given for each temporal resolution. Below, b) the number of time series available per year, c) the number of time series per length class in years and d) the number of time series with no trend, increasing or decreasing trend (Mann-Kendall trend direction) are displayed. The trend direction was switched for water table depth time series so that a rising water table (decreasing depth) is flagged as "increasing".*

The characteristics of the Earth system variables in GROW differ from their global distributions (Figure 2 & 3). The wells in GROW are disproportionately located in north mid-latitude and south mid-latitude hydrobelts (77%-91% instead of 20% globally). After Meybeck et al.[93] they are characterized by an average air temperature between 1 °C and 16 °C and medium runoff between 150 – 750 mm/year. The wells are located at lower elevations (median ground elevation of 102 m in comparison to 366 m globally) and have a median distance between perennial streams that is 1.5 km shorter in contrast to the global distribution. The main land use in GROW is characterized by a higher anthropogenic influence. While the proportion of urban areas is below 1% globally, it is very prominent in the yearly resolution data with 17%. Also, the proportion of agriculturally used land (pastures and cropland) is especially high in monthly (+ 37% fraction) and yearly data (+ 32% fraction). The distributions of the rest of the Earth system variables in GROW compared to their global distributions are given in Supplements section S2.

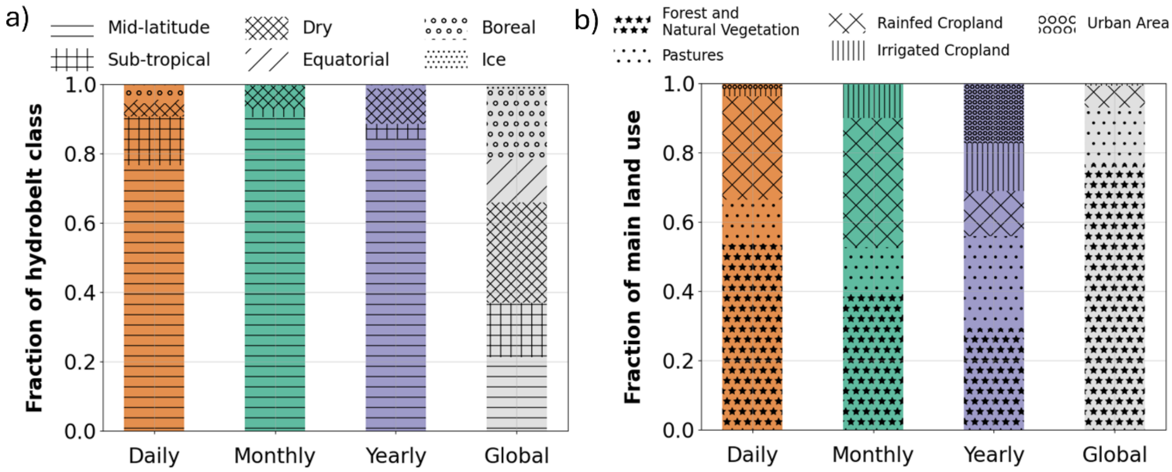

Fraction of Hydrobelt class in GROW and globally

	Daily	Monthly	Yearly	Global*
Mid Latitude	0.77	0.91	0.84	0.21
Sub Tropical	0.14	0.02	0.04	0.16
Dry	0.04	0.07	0.10	0.29
Equatorial	0.01	< 0.01	< 0.01	0.13
Boreal	0.04	< 0.01	0.01	0.20
Ice	0	0	0	0.02

Fraction of main land use in GROW and globally

	Daily	Monthly	Yearly	Global*
Forest and Natural Vegetation	0.54	0.4	0.29	0.77
Pastures	0.13	0.13	0.27	0.16
Rainfed Cropland	0.3	0.37	0.13	0.06
Irrigated Cropland	0.02	0.09	0.14	< 0.01
Urban Area	< 0.02	< 0.01	0.17	< 0.01

Figure 2 – Distribution of selected categoric Earth system variables in the GROW dataset compared with their global distribution: *This overview is showing the distribution of the following categoric Earth system variables in GROW classified by temporal resolution of the time series in comparison to the global fractions of the respective variable. The stacked bar charts show a) the fraction of hydrobelt classes after Meybeck et al.[93] and the fraction of main land use. To calculate the global distribution of the hydrobelt classes, the polygon data was transformed into a 0.05° raster. *The global distributions are derived from all pixel values in the respective raster data with area-weighting to correct for the area distortion of the WGS 84 coordinate system. The area weighting is described in more detail in the Supplements section S2.*

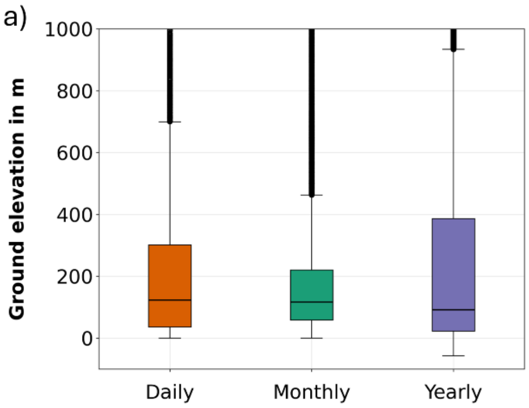

Descriptive statistics of ground elevation in m in GROW and globally

	Daily	Monthly	Yearly	Global
min	0	0	-58	- 154
median	123	116	92	366*
max	2771	3794	3847	8451

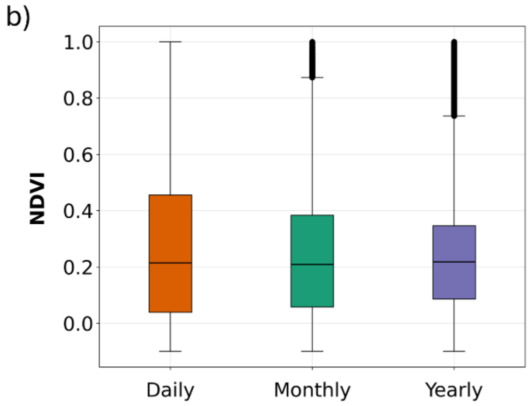

Descriptive statistics of daily average NDVI in GROW and globally

	Daily	Monthly	Yearly	Global
min	-0.1	-0.1	-0.1	-0.1
median	0.21	0.21	0.22	0.12*
max	1	1	1	1

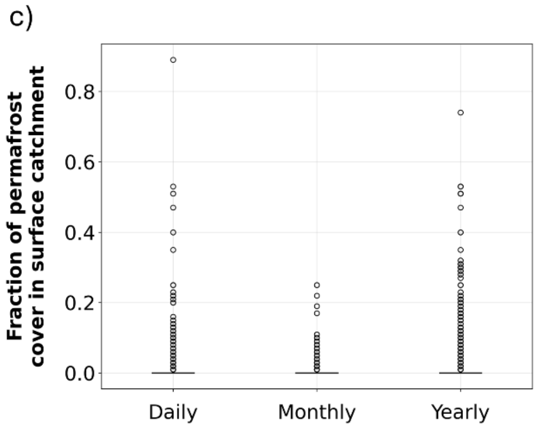

Descriptive statistics of the surface catchment's permafrost cover in GROW and globally

	Daily	Monthly	Yearly	Global
min	0	0	0	0
median	0	0	0	0*
max	0.89	0.25	0.74	1

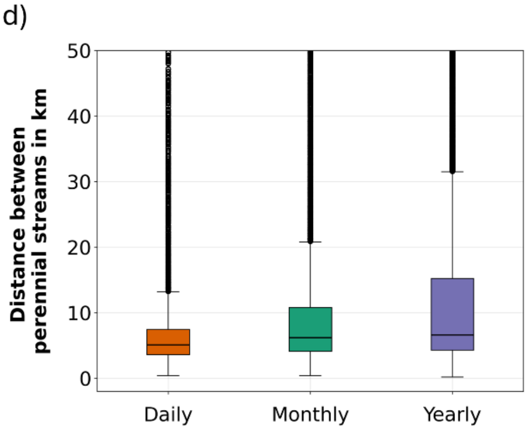

Descriptive statistics of distance between perennial streams in km in GROW and globally

	Daily	Monthly	Yearly	Global
min	0.4	0.4	0.2	0
median	5.1	6.2	6.6	7.9*
max	1215.1	1096	1215.5	1960.9

Figure 3 – Distribution of selected numeric Earth system variables in the GROW dataset compared with their global distribution: *This overview is showing the distribution of the following numeric Earth system variables in GROW classified by temporal resolution of the time series. The box plots show a) ground elevation (not full value range), b) Normalized Difference Vegetation Index (NDVI), c) permafrost cover in the surface catchment in which the well is located and d) distance between perennial streams (not full value range). Box plots show the median of a distribution as a black line inside the box. The upper and lower edges of the box are determined by the 25th and 75th percentiles (interquartile range). Whiskers indicate the farthest data point within 1.5 times the interquartile range. Outliers outside this range are displayed as dots. For readability, not all outliers are shown; thus, the tables below show the minimum, median, and maximum value of the variables in GROW for every temporal resolution in comparison to the global statistics. To calculate the global statistics of the permafrost cover, the polygon data were transformed into a 0.05° raster. *The medians of the global distributions are derived from all pixel values in the respective raster data with area-weighting to correct for the area distortion of the WGS 84 coordinate system. For the NDVI, only the global rasters of the year 2014 were used to calculate the global median. The global ground elevation raster was beforehand brought to a resolution of 30 arc seconds. The area-weighting is described in more detail in the Supplements section S2.*

TECHNICAL VALIDATION

The preprocessing of the groundwater time series ensures that the data is harmonized, gap-limited, and checked for potential measurement errors, incorrect coordinates, and duplicates. In total, 33,805 of 221,122 time series (15%) were discarded due to not meeting the quality criteria (Table 2). 8% of the time series were rejected because they were empty or contained only one record. The largest data loss in the attribute tables was due to obviously incorrect coordinates (3%). Examples of discarded time series are given in Supplements section S1. Of the remaining groundwater time series, 22,179 contain gaps (Figure 4). 40% of these time series are in a monthly resolution, and 27% are in a daily resolution. Therefore, higher-resolution time series were found to more often possess incomplete records compared to time series with yearly time steps. The median gap fraction of the time series is 3.9%. Yearly data has the highest median gap fraction (7.3%), and daily data has the lowest (0.2%) (Figure 4). The median gap length for daily data is 1.5 days; for monthly and yearly data, most of the gaps are 1 month or 1 year long (Figure 4). The total gap fraction and single gap length per well do not exceed the defined thresholds (Figure 4).

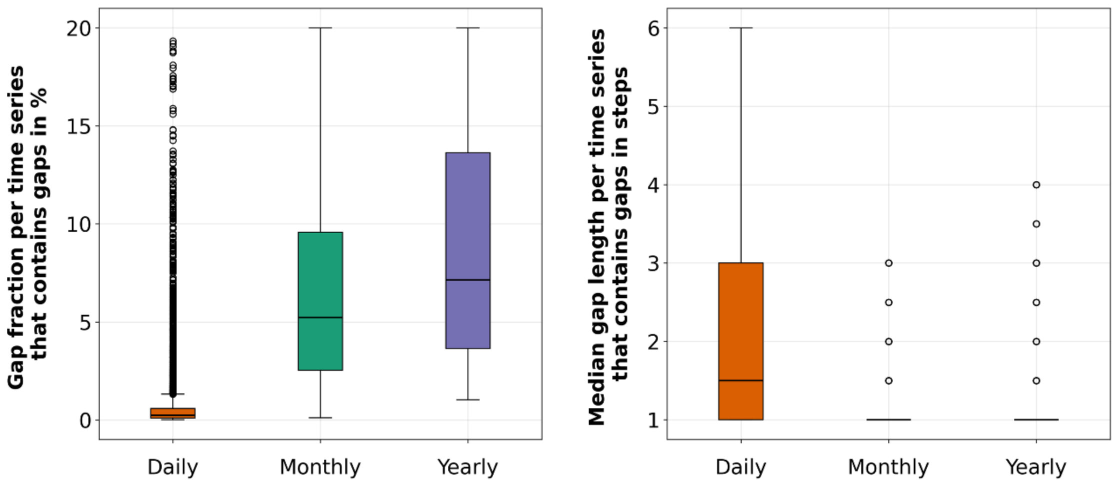

***Figure 4 – Gap fraction and median gap length per time series with gaps**: Boxplots of median gap fraction and gap length per time series, categorized by temporal resolution. Only time series in GROW that contain gaps are included (22,179). Box plots show the median of a distribution as a black line inside the box. The upper and lower edges of the box are determined by the 25th and 75th percentiles (interquartile range). Whiskers indicate the farthest data point within 1.5 times the interquartile range. Outliers outside this range are displayed as dots.*

Due to data gaps and uncertainties associated with the observed groundwater time series as well as the Earth system variables, GROW should preferably be used to analyze environmental settings that are well represented (e.g., temperate climates and low elevations, see Figure 2 & 3). GROW can additionally help to understand groundwater dynamics in the context of local to regional characteristics that are captured by the gridded data products from which the Earth system variables originate (see Table 3 & 4). The groundwater data alone can be analyzed for site-scale processes.

Regarding the groundwater observations, uncertainties arise from a lack of knowledge about the exact measurement time, metadata, and spatial data bias. As these data are provided by different data holders, the preprocessing of the groundwater data is challenging. For example, it is unclear whether the timestamp of a record indicates the exact day of measurement or an already aggregated mean for the respective period (daily, monthly, or yearly). Additionally, metadata such as the confinement of the aquifer, which is, for example, crucial for determining whether a stated water table above the ground surface is a measurement error or not, is not specified for most wells. Moreover, due to a lack of groundwater observations, the dataset is not able to represent the globally possible value ranges of all variables (Figure 2). GROW is highly biased geographically towards Northern America, Western Europe, and Australia. Additionally, groundwater observations are rather recorded at relatively shallow depths less than 10 m and in places with high anthropogenic impact (agriculture as primary land use) because wells are built where water is cost-effectively available (shallow), needed (high anthropogenic impact), and funded (wealthy countries)[105]. The GROW dataset can help detect other spatial biases towards certain climates and landscapes, and assess the consequences they have for understanding and modeling groundwater processes.

An additional source of uncertainty in GROW originates from the Earth system variables that were combined with the observed groundwater data. Uncertainties in the modelled variables arise from the oversimplification of Earth system processes and differing assumptions on how they are implemented[20,24,57,58]. Especially, human impacts are complex and difficult to quantify[59,106]. This is emphasized for the water withdrawal product in GROW, which was derived from a multi-model ensemble[107]. Wada et al.[107] found substantial differences between the three global models simulating water withdrawal trends for the industrial sector. Among other things, the authors attributed the discrepancy to differing model approaches (e.g., the distinction between electricity and manufacturing water use). Another source of uncertainty is input data[55,57,106,108]. For example, GLEAM4 primarily uses reanalysis and satellite data as simulation input[88], which pass their uncertainties on to the model output. Finally, a lack of observations[35,109], the non-applicability of local methods that are based on expert knowledge, and even computational limits[54,109] inhibit comprehensive calibration and evaluation methods. Notably, field measurements of actual evapotranspiration[110] and actual water withdrawal[107] are scarce. There are also no satellite observations as both parameters cannot be directly measured with the sensors[110,111].

There are other sources of uncertainty coming from Earth system variables that are not modelled. Satellite-based data products, such as AVHRR NDVI or MERIT DEM, have the advantage of wide temporal and spatial coverage[112]. However, satellite observations are no direct point measurements but an average characteristic over a particular spatial resolution. In this sense, the MERIT DEM lacks detailed topography, such as small lakes or levees[94]. Although reanalysis products (e.g., ERA5-Land) seem less uncertain than modelled data because they have incorporated observations, they contain their own pitfalls: They are sensitive to data availability, measurement errors, and spatial as well as temporal representativeness. Therefore, data-scarce regions and times are more uncertain[112]. The same applies to gauge-based data products like GPCC, where observation gaps are interpolated[112]. Uncertainties in categorical data like geological maps (e.g., GLiM) are not characterized by magnitude of deviation but by ambiguities in group classification. In that case, wrong mapping and deviations between regional geological maps are examples of uncertainty sources[90]. Furthermore, structural details like fault zones are neglected on the global scale[43], and there is no mapping of vertical heterogeneity[43,90,96].

Lastly, the combination of point observations with gridded data creates its own uncertainty: Commensurability errors occur when point observations are compared with grid values that represent several square kilometers. Naturally, extreme events are often not fully captured in these contexts. The greater the mismatch in (spatial) scale, the higher the commensurability error[54,112].

To reduce data uncertainty in GROW, the dataset can consequently benefit from additional groundwater time series and metadata, especially from regions that are underrepresented in the current dataset. We envision that GROW can evolve into a dynamic community dataset that continually grows and benefits from the addition of new data. As a small step in that direction, we invite the global groundwater community to contribute data to IGRAC's GGMN, which is currently the only dynamically growing global dataset of groundwater time series that offers the option to add a comprehensive set of metadata. This reduces the effort required to gather and combine data with different formats.

USAGE NOTES

The dataset, containing an attributes table and a time series table, as well as a dataset documentation can be downloaded on Zenodo: (*link will be provided in peer-reviewed manuscript*) as either a CSV or parquet file. GROW itself is published under Creative Commons Attribution Non-Commercial ShareAlike 4.0 International License (CC-BY-NC-SA 4.0). Some groundwater time series and Earth system variables are published under an individual license, but none of them is more restrictive than CC-BY-NC-SA 4.0. Please note the full license information provided in the Readme file on Zenodo. An example of use that demonstrates how the data is subset and prepared is given on GitHub (*link will be provided in peer-reviewed manuscript)* and Zenodo (*link will be provided in peer-reviewed manuscript*).

CODE AVAILABILITY

The version of the code used for the preparation of the dataset is available from Zenodo (*link will be provided in peer-reviewed manuscript*) and can be viewed and downloaded on GitHub: (*link will be provided in peer-reviewed manuscript)*. Moreover, a usage example is provided in both repositories.

ACKNOWLEDEMENTS

IG acknowledges funding for the European Research Council (ERC) Starting Grant (grant agreement No. 10104110).

GROW contains modified Copernicus Climate Change Service information 2024. Neither the European Commission nor ECMWF is responsible for any use that may be made of the Copernicus information or data it contains.

The authors are grateful to the ISIMIP3a project (https://protocol.isimip.org/#/ISIMIP3a) that provided multi-model ensemble means of domestic and industrial water withdrawal and the land use fractions.

Further, we want to thank Sara Nazari for providing data that was used in earlier stages of GROW and her advice on data products and data processing, Lina Stein for her advice on data products and an early paper draft, and Emmanuel Nyenah for his advice on data processing.

AUTHOR CONTRIBUTIONS

AB: conceptualization, investigation, methodology, data curation, validation, visualization, writing – original draft, writing – review and editing. RR: supervision, conceptualization, preparing original Draft, writing – review and editing. CRV; GL; NM: conceptualization, methodology, writing – review and editing. RC: conceptualization, advertising, writing – review and editing. MC; JF, IG; SG; AH; XH; YW; TW: conceptualization, writing – review and editing. MF: writing – review and editing.

COMPETING INTERESTS

The authors declare no competing interests.

REFERENCES

1. Margat, J. & Gun, J. van der. *Groundwater around the World: A Geographic Synopsis*. (CRC Press, Boca Raton London New York Leiden, 2013). doi:10.1201/b13977.
2. Saccò, M. *et al.* Groundwater is a hidden global keystone ecosystem. *Glob. Change Biol.* **30**, (2024).
3. *Groundwater Making the Invisible Visible*. (UNESCO, Paris, 2022).
4. Sutanudjaja, E. H. *et al.* PCR-GLOBWB 2: a 5 arcmin global hydrological and water resources model. *Geosci. Model Dev.* **11**, 2429–2453 (2018).
5. Müller Schmied, H. *et al.* The global water resources and use model WaterGAP v2.2e: description and evaluation of modifications and new features. *Geosci. Model Dev.* **17**, 8817–8852 (2024).
6. Rohde, M. M. *et al.* Groundwater-dependent ecosystem map exposes global dryland protection needs. *Nature* **632**, 101–107 (2024).
7. Kløve, B. *et al.* Groundwater dependent ecosystems. Part I: Hydroecological status and trends. *Environ. Sci. Policy* **14**, 770–781 (2011).
8. Howard, J. K., Dooley, K., Brauman, K. A., Klausmeyer, K. R. & Rohde, M. M. Ecosystem services produced by groundwater dependent ecosystems: a framework and case study in California. *Front. Water* **5**, 1115416 (2023).
9. Jasechko, S. & Perrone, D. Global groundwater wells at risk of running dry. *Science* **372**, 418–421 (2021).
10. Bierkens, M. F. P. & Wada, Y. Non-renewable groundwater use and groundwater depletion: a review. *Environ. Res. Lett.* **14**, 063002 (2019).
11. Scanlon, B. R. *et al.* Global water resources and the role of groundwater in a resilient water future. *Nat. Rev. Earth Environ.* **4**, 87–101 (2023).
12. Jasechko, S. *et al.* Rapid groundwater decline and some cases of recovery in aquifers globally. *Nature* **625**, 715–721 (2024).
13. Wada, Y., Wisser, D. & Bierkens, M. F. P. Global modeling of withdrawal, allocation and consumptive use of surface water and groundwater resources. *Earth Syst. Dyn.* **5**, 15–40 (2014).
14. Abbott, B. W. *et al.* A water cycle for the Anthropocene. *Hydrol. Process.* **33**, 3046–3052 (2019).
15. Minea, I., Boicu, D., Negm, A., Zelenakova, M. & Demirci, M. Editorial: Impact of climate changes on groundwater resources. *Front. Environ. Sci.* **13**, 1557374 (2025).
16. Haaf, E., Giese, M., Reimann, T. & Barthel, R. Data-Driven Estimation of Groundwater Level Time-Series at Unmonitored Sites Using Comparative Regional Analysis. *Water Resour. Res.* **59**, e2022WR033470 (2023).
17. Kuang, X. *et al.* The changing nature of groundwater in the global water cycle. *Science* **383**, 0630 (2024).
18. Seo, K.-W. *et al.* Abrupt sea level rise and Earth's gradual pole shift reveal permanent hydrological regime changes in the 21st century. *Science* **387**, 1408–1413 (2025).
19. Konikow, L. F. Contribution of global groundwater depletion since 1900 to sea-level rise: GROUNDWATER DEPLETION. *Geophys. Res. Lett.* **38**, (2011).

20. Condon, L. E. *et al.* Global Groundwater Modeling and Monitoring: Opportunities and Challenges. *Water Resour. Res.* **57**, e2020WR029500 (2021).
21. Reinecke, R. *et al.* Uncertainty of simulated groundwater recharge at different global warming levels: a global-scale multi-model ensemble study. *Hydrol. Earth Syst. Sci.* **25**, 787–810 (2021).
22. Intergovernmental Panel On Climate Change (IPCC). *Climate Change 2021 – The Physical Science Basis: Working Group I Contribution to the Sixth Assessment Report of the Intergovernmental Panel on Climate Change*. (Cambridge University Press, 2023). doi:10.1017/9781009157896.
23. Dubois, E. & Larocque, M. Contribution of standardized indexes to understand groundwater level fluctuations in response to meteorological conditions in cold and humid climates. *J. Hydrol.* **634**, 131105 (2024).
24. Gleeson, T., Cuthbert, M., Ferguson, G. & Perrone, D. Global Groundwater Sustainability, Resources, and Systems in the Anthropocene. *Annu. Rev. Earth Planet. Sci.* **48**, 431–463 (2020).
25. Mukherjee, A., Jha, M. K., Kim, K.-W. & Pacheco, F. A. L. Groundwater resources: challenges and future opportunities. *Sci. Rep.* **14**, 28540, s41598-024-79936–5 (2024).
26. Venegas-Quiñones, H. L. *et al.* Development of Groundwater Levels Dataset for Chile since 1970. *Sci. Data* **11**, 170 (2024).
27. Huggins, X., Gleeson, T., Villholth, K. G., Rocha, J. C. & Famiglietti, J. S. Groundwaterscapes: A Global Classification and Mapping of Groundwater's Large-Scale Socioeconomic, Ecological, and Earth System Functions. *Water Resour. Res.* **60**, e2023WR036287 (2024).
28. Rockström, J. *et al.* Safe and just Earth system boundaries. *Nature* **619**, 102–111 (2023).
29. MacDonald, A. M. *et al.* Mapping groundwater recharge in Africa from ground observations and implications for water security. *Environ. Res. Lett.* **16**, 034012 (2021).
30. Moeck, C. *et al.* A global-scale dataset of direct natural groundwater recharge rates: A review of variables, processes and relationships. *Sci. Total Environ.* **717**, 137042 (2020).
31. Wu, W.-Y. *et al.* Divergent effects of climate change on future groundwater availability in key mid-latitude aquifers. *Nat. Commun.* **11**, 3710 (2020).
32. Cuthbert, M. O. *et al.* Global patterns and dynamics of climate–groundwater interactions. *Nat. Clim. Change* **9**, 137–141 (2019).
33. West, C., Rosolem, R., MacDonald, A. M., Cuthbert, M. O. & Wagener, T. Understanding process controls on groundwater recharge variability across Africa through recharge landscapes. *J. Hydrol.* **612**, 127967 (2022).
34. Barron, O. V. *et al.* Climatic controls on diffuse groundwater recharge across Australia. *Hydrol. Earth Syst. Sci.* **16**, 4557–4570 (2012).
35. Berghuijs, W. R. *et al.* Groundwater recharge is sensitive to changing long-term aridity. *Nat. Clim. Change* **14**, 357–363 (2024).
36. Jasechko, S. *et al.* The pronounced seasonality of global groundwater recharge. *Water Resour. Res.* **50**, 8845–8867 (2014).
37. Singer, M. B. *et al.* Hourly potential evapotranspiration at 0.1° resolution for the global land surface from 1981-present. *Sci. Data* **8**, 224 (2021).
38. Fan, Y. Groundwater in the E arth's critical zone: Relevance to large-scale patterns and processes. *Water Resour. Res.* **51**, 3052–3069 (2015).
39. Gnann, S. *et al.* The Influence of Topography on the Global Terrestrial Water Cycle. *Rev. Geophys.* **63**, e2023RG000810 (2025).
40. Jasechko, S., Kirchner, J. W., Welker, J. M. & McDonnell, J. J. Substantial proportion of global streamflow less than three months old. *Nat. Geosci.* **9**, 126–129 (2016).
41. Winter, T. C. *Ground Water and Surface Water: A Single Resource*. (US Geological Survey, Denver, Col., 1999).
42. Hartmann, A., Goldscheider, N., Wagener, T., Lange, J. & Weiler, M. Karst water resources in a changing world: Review of hydrological modeling approaches: KARST WATER RESOURCES PREDICTION. *Rev. Geophys.* **52**, 218–242 (2014).

43. Gleeson, T., Moosdorf, N., Hartmann, J. & Van Beek, L. P. H. A glimpse beneath earth's surface: GLobal HYdrogeology MaPS (GLHYMPS) of permeability and porosity. *Geophys. Res. Lett.* **41**, 3891–3898 (2014).
44. Kim, J. H. & Jackson, R. B. A Global Analysis of Groundwater Recharge for Vegetation, Climate, and Soils. *Vadose Zone J.* **11**, vzj2011.0021RA (2012).
45. Winter, T. C. The Role of Ground Water in Generating Streamflow in Headwater Areas and in Maintaining Base Flow[1]. *JAWRA J. Am. Water Resour. Assoc.* **43**, 15–25 (2007).
46. Walvoord, M. A. & Kurylyk, B. L. Hydrologic Impacts of Thawing Permafrost—A Review. *Vadose Zone J.* **15**, 1–20 (2016).
47. Vincent, A., Violette, S. & Aðalgeirsdóttir, G. Groundwater in catchments headed by temperate glaciers: A review. *Earth-Sci. Rev.* **188**, 59–76 (2019).
48. Hood, J. L. & Hayashi, M. Characterization of snowmelt flux and groundwater storage in an alpine headwater basin. *J. Hydrol.* **521**, 482–497 (2015).
49. Burgess, S. S. O., Adams, M. A., Turner, N. C., White, D. A. & Ong, C. K. Tree roots: conduits for deep recharge of soil water. *Oecologia* **126**, 158–165 (2001).
50. Ilstedt, U. *et al.* Intermediate tree cover can maximize groundwater recharge in the seasonally dry tropics. *Sci. Rep.* **6**, 21930 (2016).
51. Wang, Z., Yang, Y., Chen, G., Wu, J. & Wu, J. Variation of lake-river-aquifer interactions induced by human activity and climatic condition in Poyang Lake Basin, China. *J. Hydrol.* **595**, 126058 (2021).
52. Fan, Y., Miguez-Macho, G., Jobbágy, E. G., Jackson, R. B. & Otero-Casal, C. Hydrologic regulation of plant rooting depth. *Proc. Natl. Acad. Sci.* **114**, 10572–10577 (2017).
53. Batelaan, O., De Smedt, F. & Triest, L. Regional groundwater discharge: phreatophyte mapping, groundwater modelling and impact analysis of land-use change. *J. Hydrol.* **275**, 86–108 (2003).
54. Gleeson, T. *et al.* GMD perspective: The quest to improve the evaluation of groundwater representation in continental- to global-scale models. *Geosci. Model Dev.* **14**, 7545–7571 (2021).
55. Moges, E., Demissie, Y., Larsen, L. & Yassin, F. Review: Sources of Hydrological Model Uncertainties and Advances in Their Analysis. *Water* **13**, 28 (2020).
56. Tarasova, L., Gnann, S., Yang, S., Hartmann, A. & Wagener, T. Catchment characterization: Current descriptors, knowledge gaps and future opportunities. *Earth-Sci. Rev.* **252**, 104739 (2024).
57. Beven, K. J. & Cloke, H. L. Comment on "Hyperresolution global land surface modeling: Meeting a grand challenge for monitoring Earth's terrestrial water" by Eric F. Wood et al. *Water Resour. Res.* **48**, 2011WR010982 (2012).
58. Reinecke, R. *et al.* Uncertainty in model estimates of global groundwater depth. *Environ. Res. Lett.* (2024) doi:10.1088/1748-9326/ad8587.
59. Hasan, F., Medley, P., Drake, J. & Chen, G. Advancing Hydrology through Machine Learning: Insights, Challenges, and Future Directions Using the CAMELS, Caravan, GRDC, CHIRPS, PERSIANN, NLDAS, GLDAS, and GRACE Datasets. *Water* **16**, 1904 (2024).
60. Huggins, X. *et al.* A review of open data for studying global groundwater in social-ecological systems. Preprint at https://doi.org/10.31223/X5XB07 (2025).
61. Addor, N. *et al.* Large-sample hydrology: recent progress, guidelines for new datasets and grand challenges. *Hydrol. Sci. J.* **65**, 712–725 (2020).
62. Fan, Y., Li, H. & Miguez-Macho, G. Global patterns of groundwater table depth. *Science* **339**, 940–3 (2013).
63. Kratzert, F. *et al.* Caravan - A global community dataset for large-sample hydrology. *Sci. Data* **10**, 61 (2023).
64. Cuthbert, M. O., Gleeson, T., Bierkens, M. F. P., Ferguson, G. & Taylor, R. G. Defining Renewable Groundwater Use and Its Relevance to Sustainable Groundwater Management. *Water Resour. Res.* **59**, (2023).

65. Gelsinari, S. *et al.* Nonstationary recharge responses to a drying climate in the Gnangara Groundwater System, Western Australia. *J. Hydrol.* **633**, 131007 (2024).
66. Wilkinson, M. D. *et al.* The FAIR Guiding Principles for scientific data management and stewardship. *Sci. Data* **3**, 160018 (2016).
67. Muñoz-Sabater, J. *et al.* ERA5-Land: a state-of-the-art global reanalysis dataset for land applications. *Earth Syst. Sci. Data* **13**, 4349–4383 (2021).
68. Linke, S. *et al.* Global hydro-environmental sub-basin and river reach characteristics at high spatial resolution. *Sci. Data* **6**, 283 (2019).
69. Collenteur, R. A., Moeck, C., Schirmer, M. & Birk, S. Analysis of nationwide groundwater monitoring networks using lumped-parameter models. *J. Hydrol.* **626**, 130120 (2023).
70. Jemeļjanova, M. *et al.* Modeling hydraulic heads with impulse response functions in different environmental settings of the Baltic countries. *J. Hydrol. Reg. Stud.* **47**, 101416 (2023).
71. IGRAC. The Global Groundwater Monitoring Network (GGMN). IGRAC https://doi.org/10.58154/6Z0Y-DA34 (2024).
72. Boutt, D. F. Assessing hydrogeologic controls on dynamic groundwater storage using long-term instrumental records of water table levels. *Hydrol. Process.* **31**, 1479–1497 (2017).
73. Chávez García Silva, R. *et al.* Multi-decadal groundwater observations reveal surprisingly stable levels in southwestern Europe. *Commun. Earth Environ.* **5**, 387 (2024).
74. Cuthbert, M. O. *et al.* Observed controls on resilience of groundwater to climate variability in sub-Saharan Africa. *Nature* **572**, 230–234 (2019).
75. Wagener, T. *et al.* On doing hydrology with dragons: Realizing the value of perceptual models and knowledge accumulation. *WIREs Water* **8**, e1550 (2021).
76. Lehr, C. & Lischeid, G. Efficient screening of groundwater head monitoring data for anthropogenic effects and measurement errors. *Hydrol. Earth Syst. Sci.* **24**, 501–513 (2020).
77. IGRAC. Well and monitoring data. Retrieved from https://ggis.un-igrac.org/view/well-and-monitoring-data/ (2024).
78. Jiang, X.-W., Cherry, J. & Wan, L. Flowing wells: terminology, history and role in the evolution of groundwater science. *Hydrol. Earth Syst. Sci.* **24**, 6001–6019 (2020).
79. Lyon, S. W., Grabs, T., Laudon, H., Bishop, K. H. & Seibert, J. Variability of groundwater levels and total organic carbon in the riparian zone of a boreal catchment. *J. Geophys. Res.* **116**, G01020 (2011).
80. Spearman, C. The Proof and Measurement of Association between Two Things. *Am. J. Psychol.* **15**, 72 (1904).
81. Hamed, K. H. & Ramachandra Rao, A. A modified Mann-Kendall trend test for autocorrelated data. *J. Hydrol.* **204**, 182–196 (1998).
82. Hussain, Md. & Mahmud, I. pyMannKendall: a python package for non parametric Mann Kendall family of trend tests. *J. Open Source Softw.* **4**, 1556 (2019).
83. Lin, M., Lucas, H. C. & Shmueli, G. **Research Commentary** —Too Big to Fail: Large Samples and the *p* -Value Problem. *Inf. Syst. Res.* **24**, 906–917 (2013).
84. Beck, H. E. *et al.* MSWEP V2 Global 3-Hourly 0.1° Precipitation: Methodology and Quantitative Assessment. *Bull. Am. Meteorol. Soc.* **100**, 473–500 (2019).
85. Schneider, U., Hänsel, S., Finger, P., Rustemeier, E. & Ziese, M. GPCC Full Data Monthly Version 2022 at 0.25°: Monthly Land-Surface Precipitation from Rain-Gauges built on GTS-based and Historic Data: Globally Gridded Monthly Totals. Global Precipitation Climatology Centre (GPCC) at Deutscher Wetterdienst https://doi.org/10.5676/DWD_GPCC/FD_M_V2022_025 (2022).
86. Dai, A., Fung, I. Y. & Del Genio, A. D. Surface Observed Global Land Precipitation Variations during 1900–88. *J. Clim.* **10**, 2943–2962 (1997).
87. Xu, C., Wang, W., Hu, Y. & Liu, Y. Evaluation of ERA5, ERA5-Land, GLDAS-2.1, and GLEAM potential evapotranspiration data over mainland China. *J. Hydrol. Reg. Stud.* **51**, 101651 (2024).
88. Miralles, D. G. *et al.* GLEAM4: global land evaporation and soil moisture dataset at 0.1° resolution from 1980 to near present. *Sci. Data* **12**, 416 (2025).

89. Chen, Z. *et al.* World Karst Aquifer Map (WHYMAP WOKAM). BGR , IAH, KIT, UNESCO https://doi.org/10.25928/B2.21_SFKQ-R406 (2017).
90. Hartmann, J. & Moosdorf, N. The new global lithological map database GLiM: A representation of rock properties at the Earth surface. *Geochem. Geophys. Geosystems* **13**, 2012GC004370 (2012).
91. Lehner, B. & Grill, G. Global river hydrography and network routing: baseline data and new approaches to study the world's large river systems. *Hydrol. Process.* **27**, 2171–2186 (2013).
92. Karger, D. N. *et al.* Climatologies at high resolution for the earth's land surface areas CHELSA V2.1 (current). EnviDat https://doi.org/10.16904/ENVIDAT.228.V2.1 (2021).
93. Meybeck, M., Kummu, M. & Dürr, H. H. Global hydrobelts and hydroregions: improved reporting scale for water-related issues? *Hydrol. Earth Syst. Sci.* **17**, 1093–1111 (2013).
94. Yamazaki, D. *et al.* A high-accuracy map of global terrain elevations. *Geophys. Res. Lett.* **44**, 5844–5853 (2017).
95. Amatulli, G., McInerney, D., Sethi, T., Strobl, P. & Domisch, S. Geomorpho90m, empirical evaluation and accuracy assessment of global high-resolution geomorphometric layers. *Sci. Data* **7**, 162 (2020).
96. Huscroft, J., Gleeson, T., Hartmann, J. & Börker, J. Compiling and Mapping Global Permeability of the Unconsolidated and Consolidated Earth: GLobal HYdrogeology MaPS 2.0 (GLHYMPS 2.0). *Geophys. Res. Lett.* **45**, 1897–1904 (2018).
97. Simons, G., Koster, R. & Droogers, P. HiHydroSoil v2.0 - A high resolution soil map of global hydraulic properties. (2020).
98. Huggins, X. *et al.* Overlooked risks and opportunities in groundwatersheds of the world's protected areas. *Nat. Sustain.* **6**, 855–864 (2023).
99. Volkholz, J. & Ostberg, S. ISIMIP3a landuse input data. ISIMIP Repository https://doi.org/10.48364/ISIMIP.571261.3 (2024).
100. Muñoz Sabater, J. *et al.* ERA5-land post-processed daily-statistics from 1950 to present. Copernicus Climate Change Service (C3S) Climate Data Store (CDS). https://doi.org/10.24381/cds.e9c9c792 (2024).
101. Copernicus Climate Change Service. ERA5-Land post-processed daily statistics from 1950 to present. ECMWF https://doi.org/10.24381/CDS.E9C9C792 (2024).
102. Vermote, E. & NOAA CDR Program. NOAA Climate Data Record (CDR) of AVHRR Normalized Difference Vegetation Index (NDVI), Version 5. NOAA National Centers for Environmental Information https://doi.org/10.7289/V5ZG6QH9 (2018).
103. Vermote, E. & NOAA CDR Program. NOAA Climate Data Record (CDR) of VIIRS Normalized Difference Vegetation Index (NDVI), Version 1. NOAA National Centers for Environmental Information https://doi.org/10.25921/GAKH-ST76 (2022).
104. Wada, Y. *et al.* ISIMIP3a water abstraction input data. ISIMIP Repository https://doi.org/10.48364/ISIMIP.228996 (2022).
105. Fan, Y. *et al.* Hillslope Hydrology in Global Change Research and Earth System Modeling. *Water Resour. Res.* **55**, 1737–1772 (2019).
106. Döll, P., Douville, H., Güntner, A., Müller Schmied, H. & Wada, Y. Modelling Freshwater Resources at the Global Scale: Challenges and Prospects. *Surv. Geophys.* **37**, 195–221 (2016).
107. Wada, Y. *et al.* Modeling global water use for the 21st century: the Water Futures and Solutions (WFaS) initiative and its approaches. *Geosci. Model Dev.* **9**, 175–222 (2016).
108. Müller Schmied, H. *et al.* Variations of global and continental water balance components as impacted by climate forcing uncertainty and human water use. *Hydrol. Earth Syst. Sci.* **20**, 2877–2898 (2016).
109. Yoshida, T. *et al.* Inference of Parameters for a Global Hydrological Model: Identifiability and Predictive Uncertainties of Climate-Based Parameters. *Water Resour. Res.* **58**, e2021WR030660 (2022).

110. Ezenne, G. I., Tanner, J. L., Asoiro, F. U. & Obalum, S. E. An overview of uncertainties in evapotranspiration estimation techniques. *J. Agrometeorol.* **25**, (2023).
111. Benaraba, N., Touati, F., Benyahia, S. & Yebdri, D. Jointly estimating recharge and groundwater withdrawals of the NWSAS by inverting GRACE/GRACE-FO gravity data. *Hydrol. Sci. J.* **67**, 2215–2231 (2022).
112. Sun, Q. *et al.* A Review of Global Precipitation Data Sets: Data Sources, Estimation, and Intercomparisons. *Rev. Geophys.* **56**, 79–107 (2018).